# Effect of the multivalley structure of the conduction band on helical instability in the electron-hole plasma of silicon

**V. M. Bondar, V. V. Vladimirov, N. I. Kononenko, O. G. Sarbeǐ, and A. I. Shchedrin**

*Physics Institute, Ukrainian Academy of Sciences*
(Submitted March 5, 1973)
Zh. Eksp. Teor. Fiz. **65**, 1093–1099 (September 1973)

The effect of intervalley redistribution of electrons, caused by uniaxial compression of a crystal, on the helical instability excitation criterion[1] in silicon is investigated experimentally and theoretically. The criteria for absolute or convective instability of helical waves are calculated as depending on the degree of intervalley redistribution of electrons (or pressure). Redistribution leads to an increase of ambipolar mobility. The perturbation drift therefore increases and the absolute instability criterion correspondingly increases. In the measurements of the threshold for excitation of oscillistor oscillations, an increase of the threshold by 2–3 times is observed when a pressure of $\sim 400$ kg/cm² is applied along the $\langle 100 \rangle$ direction.

1. Helical instability in a semiconductor plasma was first found by Ivanov and Ryvkin[1], who observed current instability in Ge samples placed in a sufficiently strong longitudinal magnetic field. The results of these experiments were explained by Glicksman[1] on the basis of the Kadomtsev-Nedospasov helical instability theory [1], which was developed for the positive-column plasma of a gas discharge.

The excitation of helical instability [1] in an electron-hole plasma of a semiconductor placed in a sufficiently strong longitudinal magnetic and electric field is due to the spatial separation of the fluctuations of the densities of the electrons and holes in the electron field. As a result of this separation, transverse-fluctuation components of the electric field appear and hinder the accumulation of charge. In the presence of a constant magnetic field, drift fluxes are produced in these fields and can lead to a growth of the initial density and potential perturbations. Under conditions of a multivalley structure of the conduction band (germanium, silicon, etc.), the degree of population of the valleys, owing to the anisotropy of the mobility in different valleys, can strongly influence the summary drift flux and accordingly the criterion to the excitation of helical instability in semiconductors (oscillistor).

Under ordinary conditions, when the external influences are small or nonexistent, all the valleys in Ge and Si are equivalent (are uniformly populated with electrons). We can therefore introduce for a scalar mobility all the electrons and disregard the singularities of the band structure, if the time of the inter-valley scattering is small. This approximation is used in all papers on oscillistor theory. In the case of nonuniform population of the valleys, the anisotropic mobility has a strong influence on the characteristics of the oscillistor, and it is necessary to take into account in the calculations the real band structure of the semiconductor.

In the present paper we present the results of a theoretical and experimental investigation of helical instability in silicon, when the intervalley redistribution of the electrons is due to uniaxial compression of the crystal in the $\langle 100 \rangle$ direction. The equal-energy surfaces of silicon near the bottom of the conduction band are described by six ellipsoids pairwise placed on three mutually perpendicular axes ($\langle 100 \rangle$, $\langle 010 \rangle$, $\langle 001 \rangle$). When the crystal is compressed (or stretched) in one of these directions, a maximum redistribution of the electrons among the valleys takes place (population or depletion of the valleys disposed in the strain direction)[3]. No intervalley redistribution of the electrons takes place upon compression in the $\langle 111 \rangle$ direction, and the criterion for the excitation of the helical instability is practically independent of the pressure.

2. The theoretical analysis was carried out for the case of a surface helical wave [4], inasmuch as in the stationary state the electron-hole distribution is practically uniform over the section of the sample (the surface-recombination rate is much lower than the rate of ambipolar diffusion). The calculations were performed within the framework of the two-valley model; it was assumed that the electron gas consists of two ensembles, in which the electrons have different mobilities along and across the electric field. The electron mobility in the first ensemble will be designated $\mu_{\parallel}$ and $\mu_{\perp}$ respectively in the compression direction and perpendicular to it (this ensemble is the equivalent of two valleys disposed along $\langle 100 \rangle$). In the second ensemble, corresponding to four equivalent valleys disposed along the $\langle 010 \rangle$ and $\langle 001 \rangle$ axes, the electron mobility is practically isotropic and coincides with the largest mobility ($\mu_{\perp}$ in this case). This model, as will be shown later on, describes well the real situation in silicon.

The stability was calculated for a cylindrical sample. The constant electric (**E**) and magnetic (**H**) fields are directed along the z axis (the sample was compressed in the same direction: the crystal axis $\langle 100 \rangle$ or $\langle 111 \rangle$ was oriented along z). We consider potential ($\mathbf{E}' = -\nabla\varphi'$) quasineutral ($n_I' + n_{II}' + p'$) perturbations of the type $A = A_1(r)\exp(i\omega t - im\varphi - ikz)$. The prime pertains to perturbed quantities, and the Roman number labels the valley. It was assumed that $(\mu_{\perp,\parallel}H/c)^2 \ll 1$.

With the aid of the motion and continuity equations for the electrons of each valley and for the holes we can derive equations for the perturbed electron densities ($n_{II}$, $n_{III}$), the holes ($p_1$), and the potential ($\varphi_1$):

$$n_{II}(i\omega + ik\mu_{\parallel}E) + \frac{1}{r_0^2}(\mu_{\perp}\hat{L} - \hat{k}^2\mu_{\parallel})\left(n_{0I}\varphi_1 - \frac{T}{e}n_{II}\right) + \frac{n_{II}}{\tau_{12}} - \frac{n_{III}}{\tau_{21}} = 0, \quad (1)$$

$$n_{III}(i\omega + ik\mu_{\perp}E) + \frac{\mu_{\perp}}{r_0^2}(\hat{L} - \hat{k}^2)\left(n_{0II}\varphi_1 - \frac{T}{e}n_{III}\right) + \frac{n_{III}}{\tau_{21}} - \frac{n_{II}}{\tau_{12}} = 0, \quad (2)$$

$$p_1\left(i\omega - ik\mu_h E\right) - \frac{\mu_h}{r_0^2}(L - \tilde{k}^2)\left(p_0\varphi_1 + \frac{T}{e}p_1\right) = 0, \qquad (3)$$

where

$$\hat{L} = \frac{d^2}{dx^2} + \frac{1}{x}\frac{d}{dx} - \frac{m^2}{x^2}, \qquad x = \frac{r}{r_0},$$

$r_0$ is the radius of the sample, $\tilde{k} = kr_0$, T is the carrier temperature, and $\tau_{12}$ and $\tau_{21}$ are the intervalley transition times. In the derivation of (1)–(3) we used the Einstein relation $D_i = T\mu_i/e$, where $D_i$ is the diffusion coefficient.

Recognizing that the time of the intervalley transitions in silicon, both at room temperature and at liquid-nitrogen temperature, is much shorter than the characteristic times of the oscillistor and the ambipolar diffusion times ($D_0\tau \ll r_0^2$, where $\tau = \tau_{12}\tau_{21}/(\tau_{12} + \tau_{21}) \approx 10^{-10}$ sec [5]), we can greatly simplify Eqs. (1) and (2). Using the relation

$$n_{11} = \tilde{\tau}p_1, \qquad (4)$$

which is obtained by subtracting Eqs. (1) and (2) with with allowance for the smallness of the intervalley transition times, and also the quasineutrality condition, we obtain after adding (1) and (2) the relatively simple equation

$$\tilde{p}_1[i\tilde{\omega} + iE(\bar\mu_\perp + \tilde\tau a_1)] + [\tilde{k}^2(\tilde\tau a_1 + \bar\mu_\perp) - \bar\mu_\perp \hat{L}]\tilde{p}_1$$
$$+ (\bar\mu_\perp \tilde{n}_0 \hat{L} - a_2\tilde{k}^2)\tilde\varphi_1 = 0, \qquad (4')$$

where

$$\tilde{p}_1 = \frac{p_1}{p_0}, \qquad \tilde\varphi_1 = \varphi_1\frac{e}{T}, \qquad \tilde\omega = \omega\frac{r_0^2}{D_h}, \qquad \tilde{E} = E\frac{kr_0^2e}{T},$$

$$\tilde{n}_0 = \tilde{n}_{0\mathrm{I}} + \tilde{n}_{0\mathrm{II}}, \qquad \tilde{n}_{0\mathrm{I, II}} = n_{0\mathrm{I, II}}/p_0, \qquad a_1 = \bar\mu_\parallel - \bar\mu_\perp,$$
$$a_2 = \bar\mu_\parallel\tilde{n}_{0\mathrm{I}} + \bar\mu_\perp\tilde{n}_{0\mathrm{II}}, \qquad \bar\mu_{\parallel, \perp} = \mu_{\parallel, \perp}/\mu_h,$$

$$\tilde\tau = \frac{1}{1 + \tau_{21}/\tau_{12}} \approx \frac{1}{1 + n_{0\mathrm{II}}/n_{0\mathrm{I}}} = \frac{n_{0\mathrm{I}}}{n_0}, \qquad n_0 = n_{0\mathrm{I}} + n_{0\mathrm{II}}.$$

Relation (4) has a simple meaning: the fluctuations of the electron density in each of the valleys are proportional to the stationary concentrations of the electrons in these valleys. Equations (3) and (4) are the starting points for the subsequent calculations.

The boundary conditions can be obtained by integrating Eqs. (3) and (4') over an infinitesimally thin layer near the surface of the sample. For a low rate of surface recombination, these conditions correspond to the vanishing of the radial hole flux and the summary electron flux on the surface of the sample:

$$\frac{d\tilde\varphi_1}{dx}\tilde{n}_0 - \frac{d\tilde{p}_1}{dx} + im\tilde{H}\bar\mu_\perp(\tilde{n}_0\varphi_1 - p_1)|_{x=1} = 0,$$

$$\frac{d\tilde\varphi_1}{dx} + \frac{d\tilde{p}_1}{dx} - im\tilde{H}(\tilde\varphi_1 + \tilde{p}_1)|_{x=1} = 0, \qquad (5)$$

where $\tilde{H} = \mu_h H/c$. The solutions of (3) and (4') are

$$\tilde{p}_1 = c_1 I_m(y_1 x) + c_2 I_m(y_2 x),$$

$$\tilde\varphi_1 = -\frac{1}{b_6}[c_1 I_m(y_1 x)(b_5 + b_7 y_1^2) + c_2 I_m(y_2 x)(b_5 + b_7 y_2^2)], \qquad (6)$$

where $y_{1,2} = \sqrt{z_{1,2}}$ are the solutions of the quadratic equation

$$b_3 b_7 z^2 - z(b_2 b_7 - b_3 b_5 + b_4 b_6) - b_1 b_6 - b_2 b_5 = 0.$$

Here

$$b_1 = i\tilde\omega(1 - \bar\mu_\perp\tilde{n}_0) + iE[\bar\mu_\perp(1 + \tilde{n}_0) + \tilde\tau a_1] + \tilde{k}^2[\bar\mu_\perp(1 - \tilde{n}_0) \mp \tilde\tau a_1],$$
$$b_2 = \tilde{k}^2(\bar\mu_\perp\tilde{n}_0 + a_2), \qquad b_3 = 2\bar\mu_\perp\tilde{n}_0, \qquad b_4 = -\bar\mu_\perp(1 - \tilde{n}_0),$$
$$b_5 = i\tilde\omega(1 + \bar\mu_\perp\tilde{n}_0) + iE[\bar\mu_\perp(1 - \tilde{n}_0) + \tilde\tau a_1] + \tilde{k}^2[\bar\mu_\perp(1 + \tilde{n}_0) + \tilde\tau a_1],$$
$$b_6 = \tilde{k}^2(\bar\mu_\perp\tilde{n}_0 - a_2), \qquad b_7 = -\bar\mu_\perp(1 + \tilde{n}_0),$$

$I_m(y_{1,2}x)$ is a Bessel function of first order and of imaginary argument.

Substituting the solutions (6) in the boundary conditions (5) we can obtain, after eliminating the integration constants ($c_1, c_2$), the dispersion equation

$$y_1 y_2(y_1^2 - y_2^2)\frac{b_7^2}{\bar\mu_\perp}I_m'(y_1)I_m'(y_2) - im\tilde{H}[y_1 I_m'(y_1)I_m(y_2) - y_2 I_m'(y_2)I_m(y_1)]$$

$$\times\left[b_6 b_7\frac{1 + \tilde{n}_0}{\tilde{n}_0(1 + \bar\mu_\perp)} + \frac{\tilde{n}_0(1 + \bar\mu_\perp)}{b_6}(b_5^2 + b_7^2 y_1^2 y_2^2)\right]$$

$$+ b_5(1 + \bar\mu_\perp)(1 - \tilde{n}_0) + \frac{(1 - \bar\mu_\perp\tilde{n}_0)(\bar\mu_\perp - \tilde{n})}{\tilde{n}_0(1 + \bar\mu_\perp)}\Big] + im\tilde{H}y_1 y_2[y_1 I_m(y_1)I_m'(y_2)$$

$$- y_2 I_m(y_2)I_m'(y_1)][b_5\tilde{n}_0(1 + \bar\mu_\perp) + b_7(1 - \bar\mu_\perp\tilde{n}_0)] + im\tilde{H}[y_2^3 I_m(y_1)I_m'(y_2)$$

$$- y_1^3 I_m(y_2)I_m'(y_1)][b_5\tilde{n}_0(1 + \bar\mu_\perp) + b_7(\bar\mu_\perp - \tilde{n}_0)] = 0. \qquad (7)$$

Using the expansion of the Bessel functions in the terms of the small argument, we analyzed this relation for the helical mode. We confined ourselves to the first two terms of the expansion, since allowance for the next terms does not influence the threshold characteristics of the oscillistor. We present the principal results.

The instability criterion (Im $\omega < 0$) is given by

$$EH > \frac{3k_u c D_h}{m\mu_h^2}\frac{(1 + \bar\mu_\perp\tilde{n}_0)[\bar\mu_\perp(2 + \tilde{n}_0) + \tilde\tau a_1 + a_2]}{\bar\mu_\perp\tilde{n}_0(1 + \bar\mu_\perp)(1 + \bar\mu_\perp + \tilde\tau a_1)}; \qquad (8)$$

the value of the wave vector at which the excitation criterion is minimal is

$$k_u^2 = \frac{1}{r_0^2}\frac{8}{3}\frac{\bar\mu_\perp(1 + \tilde{n}_0)}{\bar\mu_\perp(2 + \tilde{n}_0) + \tilde\tau a_1 + a_2}; \qquad (9)$$

the oscillation frequency near the excitation threshold is

$$\omega_u = k_u\mu_h E\frac{\bar\mu_\perp(\hat{n}_0 - 1) - \tilde\tau a_1}{1 + \bar\mu_\perp\tilde{n}_0}. \qquad (10)$$

Expression (10) is valid when the ambipolar mobility differs from zero:

$$\mu_a = \mu_h\frac{\bar\mu_\perp(\tilde{n}_0 - 1) - \tilde\tau a_1}{1 + \bar\mu_\perp\tilde{n}_0} \neq 0.$$

If $\mu_\perp = \mu_\parallel$, then expressions (8)–(10) coincide with the results obtained assuming scalar mobility of the electrons [4].

The criteria for absolute and convective instability of the helical modes are the same if $\mu_a = 0$ [4], inasmuch as in this case there is no drift of the perturbations along the electric field. If $\mu_a \neq 0$, then the criterion (8) coincides with the condition for the onset of convective instability [4] or of spatial amplification (along the z axis) of the helical waves (Im $k > 0$) at the threshold frequency. The criterion of absolute instability of helical waves is more stringent. For this instability to occur it is necessary that the drift flux causing this instability be larger than the summary diffusion flux and the flux due to the ambipolar drift along the electric field that leads to a drift of the perturbations. The criterion for absolute instability, obtained in analogy with [4] (the linear response of the system with dispersion (7) to a perturbation in the form of a $\delta$-function in space and in time) is given by

$$E^2 H^2 > \frac{64c^2 D_h^2}{r_0^2\mu_h^4(1 + \bar\mu_\perp)^2[\bar\mu_\perp(1 + \tilde{n}_0) + \tilde\tau a_1]^2}$$

$$\qquad (11)$$

$$\times\left\{\frac{3}{2}\bar\mu_\perp(1 + \tilde{n}_0)[\bar\mu_\perp(2 + \tilde{n}_0) + \tilde\tau a_1 + a_2] + \frac{9}{64}\left(\frac{r_0 E\mu_h}{D_h}\right)^2[\bar\mu_\perp(\tilde{n}_0 - 1) - \tilde\tau a_1]^2\right\}.$$

This expression was obtained in the approximation $|\bar\mu_\perp(\tilde{n}_0 - 1) - \tilde\tau a_1| \ll 1$. Inasmuch as $(r_0 E\mu_h/D_h)^2 \gg 1$, the criterion (11) depends strongly on the value of the ambipolar mobility. The corresponding threshold value of HE
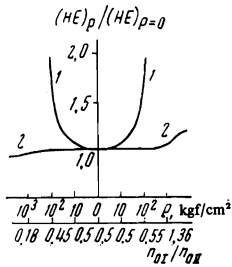
FIG. 1. Theoretical plots of the criterion of absolute instability (curve 1) and convective instability (curve 2) of helical waves vs. the degree of intervalley redistribution of the electrons. On the left—stretching, on the right—compression.

is minimal when $\mu_a = 0$. Within the framework of the model used in the present paper, this corresponds to $\tilde{n}_0 = 11/15$ if $\mu_\perp/\mu_\parallel = 5$ (see [5] for the case of silicon). With increasing $|\mu_a|$, when the crystal is compressed or stretched, the threshold for the excitation of the absolute instability increases because the ambipolar drift of the perturbation becomes stronger. The criterion for the excitation of the convective instability (8) does not depend on the ambipolar mobility and should decrease when the crystal is stretched, since the electrons move into the valley with the larger mobility in the direction of the electric field.

Figure 1 shows the calculated threshold plots of $(HE)_p/(HE)_{p=0}$ of the absolute instability (curve 1) and convective instability (curve 2) as functions of the degree of the intervalley redistribution ($n_{0I}/n_{0II}$) and of the pressure P for an injection level $\tilde{n}_0 = 11/15$. Within the framework of the two-valley model, zero pressure corresponds to $n_{0I}/n_{0II} = \frac{1}{2}$. The ratio of the concentration in the valleys was connected with the pressure in the following manner [5]

$$\frac{n_{0I}}{n_{0II}} = \frac{1}{2} \exp \frac{\Sigma_u P}{(c_{11} - c_{12})kT},$$

where $\Sigma_u = 8$ eV for silicon (the deformation-potential constant), $c_{11} = 1.67$ dyne/cm$^2$, and $c_{12} = 0.65 \times 10^{12}$ dyne/cm$^2$. As seen from this figure, even at a slight redistribution the excitation threshold of the absolute instability increases sharply, regardless of the deformation direction, this being due to the increase of $|\mu_a|$. The criterion of convective instability depends much less on the degree of redistribution of the electrons (pressure); upon compression, the amplification threshold increases somewhat, since the electrons move into the valley with low mobility along the electric field, and decreases in the case of tension.

3. The experiments were performed at liquid-nitrogen pressure in order, on the one hand, to increase the carrier mobility, and on the other ensure a sufficient transfer of the electrons under small compression. The samples were oriented in a definite direction ($\langle 111 \rangle$, $\langle 100 \rangle$) and were cut from a p-type single crystal with $\rho(300°K) = 1900$ $\Omega$-cm; the hole density $p_0 = 5 \times 10^{12}$ cm$^{-3}$ was determined from measurements of the Hall effect. The sample dimensions were $1 \times 1 \times 10$ mm. To ensure a low surface-recombination rate, the samples were etched in a mixture of hydrofluoric and nitric acids (ratio 1:8) at $t = 0°C$. The samples had four contacts each. The end contacts and one of the lateral contacts were ohmic and were prepared by fusing-in pure aluminum at 700°C in a vacuum in a $10^{-5}$ mm Hg vacuum. The lateral injecting contact was produced by fusing-in gold with 0.5% antimony added at 550°C in the same vacuum.

The schematic diagram of the installation for the measurement of the influence of uniaxial compression on the oscillistor effect is shown in Fig. 2a. The uni-
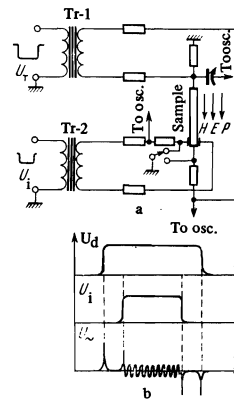


FIG. 2



FIG. 3

FIG. 2. Schematic diagram of installation (a) and time schedule (b) of the drawing ($U_d$) and injecting ($U_i$) fields. $U_\sim$—typical waveform of resultant oscillations.

FIG. 3. Experimental (1, 2) and theoretical (3-5) plots of the absolute-instability criterion vs. pressure for different injection levels.
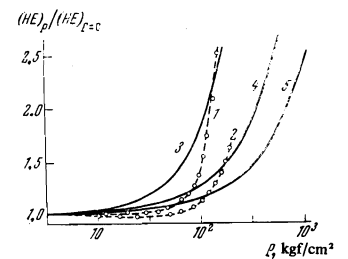
axial compression was produced by an ordinary lever-actuated press. To prevent noticeable heating of the sample, pulsed electric fields were used. The drawing[1] field ($U_d$) had a duration 130–150 sec, and the injecting field ($U_i$), 80–100 sec. The time schedules of the drawing and injecting field, and also a typical waveform ($U_\sim$) of the resultant oscillations ($f \approx (1-2) \times 10^6$ Hz) are shown in Fig. 2b. This sequence of turning on the drawing and injecting fields makes it possible to monitor the onset of oscillistor oscillations when the injecting field is turned on. The magnetic field ranged from 1–5 kOe, while the drawing electric field was $\approx 120$ V/cm (and was practically constant). The injection level was maintained constant during the course of the measurements and was chosen such that the amplitude was maximal in the absence of compression.

Figure 3 shows the experimental plots of the generation threshold against the pressure for injection levels $\tilde{n}_0 \approx 0.7$ (curve 1) and $\tilde{n}_0 \approx 0.8$ (curve 2). Even a very slight redistribution of the electrons ($P = 100$ kgf/cm$^2$; $n_{0I}/n_{0II} \approx 0.54$) initiates a rapid growth of the threshold value of HE. Curves 3, 4, and 5 correspond to the theoretical pressure dependences of the absolute-instability criterion (11) for $n_0 = 11/15$, $12/15$, and $13/15$, respectively.

It is seen from the foregoing data that the results of calculations in the two-valley-model approximation agree well with the experimental data, viz., a sharp increase in the threshold value of HE with increasing pressure is observed for the crystallographic direction $\langle 100 \rangle$, whereas for the direction $\langle 111 \rangle$ the values of the threshold fields remain practically unchanged.

---

[1] By drawing and injection fields are meant the fields between the end and lateral contacts, respectively.

[1] Yu. L. Ivanov and S. M. Ryvkin, Zh. Tekh. Fiz. **28**, 774 (1958) [Sov. Phys.-Tech. Phys. **3**, 722 (1958)].

[2] M. Glicksman, Sol. State Phys. **26**, 275 (1971).

[3] R. W. Keyes, Sol. State Phys. **11**, 149 (1960).

[4] C. E. Hurwitz, Mc. Whorter, Phys. Rev. **134A**, 1033 (1964).

[5] M. Asche, B. L. Boichenko, V. M. Bondar, and O. G. Sarbey, Phys. Stat. Scol. **44**, 173 (1971).

Translated by J. G. Adashko
111